Simple luminosity normalization of greenness, yellowness and redness/greenness for comparison of leaf spectral profiles in multi-temporally acquired remote sensing images

RYOICHI DOI

Graduate School of Agricultural and Life Sciences, The University of Tokyo, 1-1-1 Yayoi, Bunkyo-ku, Tokyo 113-8657, Japan

(Fax, 81-3-5841-1606; Email, roird2000@yahoo.com)

Observation of leaf colour (spectral profiles) through remote sensing is an effective method of identifying the spatial distribution patterns of abnormalities in leaf colour, which enables appropriate plant management measures to be taken. However, because the brightness of remote sensing images varies with acquisition time, in the observation of leaf spectral profiles in multi-temporally acquired remote sensing images, changes in brightness must be taken into account. This study identified a simple luminosity normalization technique that enables leaf colours to be compared in remote sensing images over time. The intensity values of green and yellow (green+red) exhibited strong linear relationships with luminosity (R^2>0.926) when various invariant rooftops in Bangkok or Tokyo were spectral-profiled using remote sensing images acquired at different time points. The values of the coefficient and constant or the coefficient of the formulae describing the intensity of green or yellow were comparable among the single Bangkok site and the two Tokyo sites, indicating the technique's general applicability. For single rooftops, the values of the coefficient of variation for green, yellow, and red/green were 16% or less (n=6−11), indicating an accuracy not less than those of well-established remote sensing measures such as the normalized difference vegetation index. After obtaining the above linear relationships, raw intensity values were normalized and a temporal comparison of the spectral profiles of the canopies of evergreen and deciduous tree species in Tokyo was made to highlight the changes in the canopies' spectral profiles. Future aspects of this technique are discussed herein.

[Doi R 2012 Simple luminosity normalization of greenness, yellowness and redness/greenness for comparison of leaf spectral profiles in multi-temporally acquired remote sensing images. *J. Biosci.* **37** 723–730] **DOI** 10.1007/s12038-012-9241-3

1. Introduction

Leaf colour is an indicator of plant condition. As a component of the red-green-blue (RGB) colour model, green is the colour of chlorophyll, which generates energy (Shuvalov 2007). The greenness of leaves changes in response to various environmental changes. In autumn, the leaves of a variety of deciduous species turn reddish brown, orange or yellow (Lev-Yadun and Gould 2007). The loss of the colour green is a sign of leaf senescence. In addition to seasonal changes, some types of nutritional deficiencies such as nitrogen deficiency (Pagani *et al*. 2009) result in a yellowish leaf colour. An abnormality in leaf colour indicates a disorder of the plant body caused by above-ground stresses (Sicher 1999) or poor soil conditions (Olszewska *et al*. 2008). It is thus evident that observation of leaf colour enables suitable plant management measures (Van Niel and McVicar 2004).

Over a wide area, it is difficult to observe all of the leaves' colours although reliable *in situ* measurement techniques exist (Balasubramanian *et al.* 2000). Furthermore, an abnormal leaf colour is often unevenly and irregularly distributed over a single area (Doi and Mahaut 2006). Therefore, the remote sensing of vegetation assists in the management of fields (Spurr 1948). With the help of remote sensing technologies, many researchers have been making efforts to

Keywords. Public availability and feasibility; rooftop invariants; remote sensing image; spatio-temporal variability of leaf spectral profile; temporal variation of brightness

Published online: 11 August 2012

establish methods to observe vegetation as an assembly of plants and leaves (Newton *et al.* 2009). They have successfully realized the remote sensing of natural vegetation and other areas such as agricultural fields. Discrimination of areas with different land covers has also been achieved. In the regional-scale observation of vegetation and other areas, discrimination and land-cover mapping have already been relatively well established (Lu and Weng 2007). Thus, the more precise observation of vegetation (i.e. canopies and leaves) is sought. As indicated by some studies on land-cover mapping at smaller scales (Bunting and Lucas 2006; Doi and Ranamukhaarachchi 2010), observational accuracy can be improved using the latest artificial satellites and sensors or *in situ* methods for aerial photographing. Recent developments in remote sensing technologies can even provide textural information on canopies. These precise remote sensing technologies enable the recognition of single tree branches and their leaves.

However, the brightness of the imaging targets varies with image acquisition time. As such, in the observation of leaf colours (spectral profiles) in remote sensing images acquired over a period of time, changes in the brightness of a remotely captured land area must be taken into account (Hadjimitsis *et al.* 2009). The difficulty in the normalization of brightness in multiple remote sensing images acquired at different time points has been recognized (Schott *et al*. 1988). A major cause of this difficulty is the absence of correlations among bands that may be used for the spectral profiling of leaves among different time points (Hayes and Sader 2001). A great deal of efforts have been made to normalize the brightness of all images acquired at different time points, considering all remote sensing bands, although adjustment of the entire area of a single remote sensing image is difficult due to the absence of correlations (Hadjimitsis *et al*. 2009).

As a single piece of information from remote sensing images, greenness can be extracted to reveal the physiological conditions of leaves, regardless of whether or not there are correlations with other colour variables. This simple extraction and quantitative use of information relating to the greenness of pixels in remote sensing images have not yet been reported. This study explores the relationships between the varying brightness and the intensity of red-green-blue (RGB) or cyan-magenta-yellow-black (CMYK) colour components in true colour remote sensing images. Adobe Photoshop was used as one of the tools to report both the RGB spectral profiles and the brightness of single pixels in the image data (Doi *et al*. 2010) provided by Google Earth. The first objective of this study was to find a normalization technique to enable the comparison of the spectral profiles of leaves shown in true colour remote sensing images acquired at multiple time points. As invariant spectral standards, multiple rooftops with different spectral profiles were used. The second study objective was to demonstrate the applicability of the normalization technique by comparing the spectral profiles of tree leaves at different time points and by identifying the trends in the seasonal changes in the spectral profile of leaves. Canopies of Himalayan cedar, keyaki (Japanese zelkova), ginkgo and Japanese stone oak on a university campus in Tokyo were profiled.

2. Methods

2.1 *Site description*

In this study, rooftops in remote sensing images of Bangkok, Thailand, and Tokyo, Japan, were used as invariant standards. The Bangkok site was located in the Chatuchak district of Bangkok (13° 50′ 01.42″ N, 100° 34′ 39.20″ E). At the Bangkok site, a red, an orange, a blue, a green and a purple rooftop were chosen based on visual confirmation at the site. The remote sensing images were true colour images, which enabled visual confirmation of the aforementioned rooftops. In Tokyo, two sites were chosen, both of which were in the Bunkyo district. Hereafter, the sites will be referred to as Tokyo 1 (35° 43′ 12.03″ N, 139° 44′ 54.18″ E) and Tokyo 2 (35° 42′ 45.54″ N, 139° 45′ 22.21″ E). For each of the Tokyo sites, a red, a green, a blue, a cyan and a yellow rooftop were visually chosen, as in the case of the Bangkok site. For each site, all rooftops were located within a 1 km×1 km square. The Tokyo 2 site included the University of Tokyo's campus (figure 1), which had canopies of Himalayan cedar (*Cedrus deodara*), keyaki (*Zelkova serrata*), ginkgo (*Ginkgo biloba*) and Japanese stone oak (*Lithocarpus edulis*).

2.2 *Spectral profiling of rooftops and tree canopies*

In this study, true colour remote sensing images provided by Google Earth were used. The remote sensing images were captured by the satellite, Quickbird or GeoEye. For each site, all rooftops were located within a single remote sensing image. For the Tokyo 2 site, the five rooftops and canopies were recognized in a single remote sensing image. The Google Earth images were captured six times between 10 Jan 2005 and 31 Jan 2010 (Bangkok), 8 times between 9 Jan 2003 and 1 Jan 2007 (Tokyo 1), and 11 times between 1 Jan 1997 and 6 June 2010 (Tokyo 2). No clouds were observed in the remote sensing images. For rooftop spectral profiling and analysis, in the Google Earth window, a virtual altitude of 900 m above ground was chosen when copying the remote sensing images from the Google Earth window using the 'copy image' function. The original multispectral image included data on RGB colour intensity and panchromatic grayscale values. When the image was copied from the Google Earth window, the data regarding the values of the RGB colour intensity were retained. The image data was

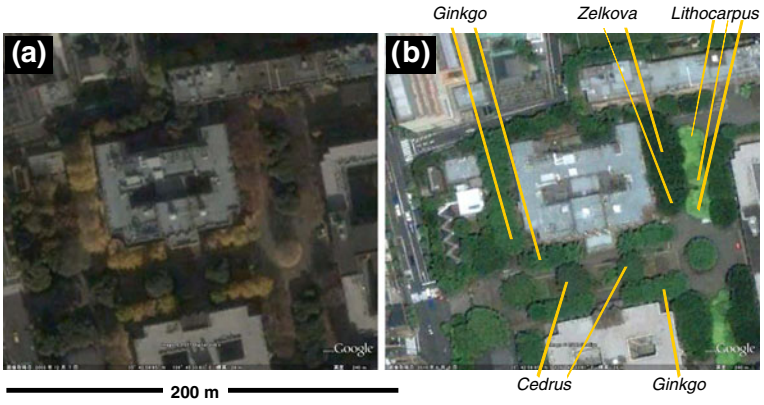

Figure 1. Remote sensing images of the university campus in the Tokyo 2 site. The left image (**a**) was acquired on 7 December 2003, and the right image (**b**) on 6 June 2010. The species names indicate the spectral-profiled canopies.

then pasted into a new file window of Adobe Photoshop 7.0. In the Adobe Photoshop window, a single pixel represented an area of 1 m^2. At least 16 pixels per rooftop were profiled in the RGB mode and then averaged. For each RGB colour component, a value between 0 (darkest) and 255 (saturated and most colourful) was shown (Doi 2012). As a measure of brightness, luminosity was also read for the pixels and was averaged as above. In the same way, cyan, magenta, and yellow intensity values were also read in the CMYK mode. For profiling tree canopies (figure 1), in the Google Earth window, a virtual altitude of 240 m above ground was chosen when copying the images. A single pixel represented an area of 361 cm^2. Three hundred or more pixels per canopy were profiled in the RGB or CMYK mode and then averaged. Three *Ginkgo*, two *Zelkova*, three *Lithocarpus* and two *Cedrus* canopies were profiled. The canopy images were taken on 2 Jun 2002, 7 Dec 2003, 15 Sep 2004, and 6 Jun 2010. Shaded areas were avoided in profiling rooftops and canopies. In profiling *Ginkgo* canopies, female trees were chosen.

2.3 *Data analyses*

Yellow is also an important colour in leaf observation (Adams *et al.* 1999). Therefore, in addition to the Y of the CMYK colour model, the intensity of RGB yellow was calculated (Smith 1999) as

$$\text{RGB yellow} = \text{G} + \text{R} \quad (1)$$

As a measure of the relative intensity of R to G, the R/G value was also calculated (Kondo *et al.* 2000). Using the statistical software SPSS 10.0.1 (SPSS Inc.), a linear regression analysis of the luminosity and the intensity of the RGB or CMYK colour component was performed. To examine the significance of tree species and image acquisition time as sources of variation in the canopy spectral profile, repeated measures analysis of variance was performed using the same SPSS software. A least significant difference *t*-test was performed to examine the significant differences between the means.

3. Results and discussion

3.1 *Relationships between brightness and intensity of colour components*

Table 1 presents the linear relationships between the luminosity and intensity of colour components of the RGB and CMYK models derived from the rooftop profiling. Among the single colour components, RGB yellow had the greatest R^2 value (R^2>0.954) followed by G (R^2>0.926). The other colour components were found to be unreliable for the spectral profiling of rooftops (R^2<0.796). Similar trends were observed among the three sites. The linear relationship between G and luminosity was as previously discussed by Kirk *et al.* (2009).

In the image processing with Adobe Photoshop, luminosity is determined (Handschuh *et al.* 2010) as

$$\text{Luminosity} = 0.3\text{R} + 0.59\ \text{G} + 0.11\ \text{B} \quad (2)$$

G has the greatest weight of 0.59, but the linear relationship between luminosity and the intensity value of G could not necessarily be significant. Red, orange and yellow rooftops have great intensity values of R, while blue and purple roof tops do of B. As the linear relationship between luminosity and R or B was less significant (table 1), G could have an insignificant relationship with luminosity. However, among the RGB colour components, G had the most significant linear relationship with luminosity. This significant linear relationship, as well as table 1, indicates the absence of correlations among the axes of the

Table 1. Linear relationships between luminosity and color components derived from profiling of rooftops

Spectral variable	Bangkok			Tokyo 1			Tokyo 2		
described	Coefficient*	Constant*	R^2	Coefficient	Constant	R^2	Coefficient	Constant	R^2
R	1.27	−22.1	0.787	1.04	−0.56	0.694	1.11	−13.6	0.788
G	0.97	−0.54	0.927	1.02	−2.66	0.948	0.99	−2.53	0.952
B	0.42	−65.3	0.328	0.82	−15.5	0.623	0.77	−23.5	0.663
RGB yellow (R+G)	2.24	−23.7	0.967	2.04	−1.66	0.955	2.10	−11.0	0.971
C	0.99	−17.4	0.480	0.67	49.0	0.380	0.99	3.47	0.625
M	0.88	−22.5	0.752	0.83	−39.4	0.795	0.81	−45.0	0.692
Y	0.02	−133	< 0.001	0.50	−70.7	0.331	0.44	−78.7	0.254

*Intensity expressed as a digital count number between 0 and 255 = coefficient x luminosity + constant

RGB colour components in the colour space (Hayes and Sader 2001). Thus, the theoretically proven linear relationship between G and luminosity (Kirk *et al*. 2009) was experimentally demonstrated.

The linear relationship between luminosity and RGB yellow was unexpected. This was interesting because CMYK yellow had no linear relationship with luminosity. One possible explanation is the difference between RGB yellow and CMYK yellow caused by a minor peak in the red spectrum at around 410 nm that does not exist in the CMYK yellow spectrum (Smith 1999). This may make the axes of RGB and CMYK yellowness have different directions in the colour space. The method in the current study extracts single colour components (R and G), while the intensity value of RGB yellow is obtained by summing those of extracted R and G (Smith 1999). A colourful greenish colour given by only a single RGB colour component (R=0, G=255, B=0) can be approximated as a CMYK colour (C=161, M=0, Y=255, K=0). This indicates that the greenish colour contains a significant yellow component. Likewise, a colourful reddish colour (R=255, G=0, B=0) also has a significant yellow component (C=0, M=252, Y=255, K=0). Because the obtained RGB yellow had a more significant linear correlation with luminosity than the other RGB and CMYK components, the axis of luminosity was thought to exist between those of R and G on a plane in the colour space.

Another interesting thing was that the statistics for G and RGB yellow indicate the possibility of multiple site comparison as the values of the coefficient or constant were similar among the three sites. Because five rooftops were profiled and because of the aforementioned linear relationships, for each image acquisition time, raw values of G and RGB yellow were normalized using the following equation:

$$\text{Raw value} \times 100 \Big/ \left[\sum (\text{luminosity for single rooftop}) / 5\right] = \text{Luminosity100} - \text{normalized value} \quad (3)$$

3.2 *Normalization of raw observations*

Table 2 presents the luminosity100-normalized profiles of the rooftops. In addition to normalized G and RGB yellow values, normalized R/G values are shown. The values of the coefficient of variation for each rooftop were up to 17%. Large G values, for example, for the cyan rooftops in the Tokyo sites, indicate a high degree of saturation of G, and thus high colourfulness. In contrast, a small G value indicates that the rooftop was dark, as seen for the green rooftops at the Tokyo sites. The values of the coefficient of variation for R/G were comparable to those of Green and RGB yellow. As a measure of accuracy, the range of the coefficient of variation implies that, at worst, the spectral profiling based on the current normalization technique did not underperform the *in situ* technique for the measurement of greenness using a chlorophyll meter SPAD-502 (Steele *et al.* 2008; Coste *et al.* 2010). The red, orange and yellow rooftops had relatively large R/G values. Therefore, in describing the spectral profiles of leaves, R/G was expected to be a spectral variable that indicated the relative concentration of reddish pigments to chlorophyll. In a regional-scale remote sensing study, Yang *et al.* (2008) reported that R/G demonstrated an accuracy not less than the well-investigated indices, including the normalized difference vegetation index. Hence, the accuracy of G is also expected to be at least comparable to that of well-established indices for the remote sensing of vegetation based on panchromatic information.

3.3 *Seasonal and between-species variations of leaf spectral profile*

Changes in the spectral profiles of canopies on the university campus are summarized in table 3. As sources of variations of G, R/G, and RGB yellow, tree species, image acquisition time and the interaction (tree species × image acquisition time) were significant (p=0.002 or smaller) according to repeated measures analysis of variance. Seasonal changes

Table 2. Luminosity 100-normalized spectral profiles of the rooftops and validation of normalized green (G), R/G and RGB yellow values

Normalized spectral variable	Visual rooftop appearance	Bangkok			Visual rooftop appearance	Tokyo 1			Tokyo 2		
		Mean	SD*	CV **(%)		Mean	SD	CV (%)	Mean	SD	CV (%)
G	Red	74	9	13	Red	85	9	10	83	10	12
	Orange	131	13	10	Green	76	12	16	81	7	8
	Green	106	7	6	Blue	83	7	9	81	7	9
	Blue	85	6	7	Cyan	146	10	7	132	7	5
	Purple	86	6	7	Yellow	106	8	7	128	10	8
R/G	Red	1.61	0.26	16	Red	1.41	0.10	7	1.40	0.15	11
	Orange	1.22	0.09	8	Green	0.89	0.08	9	0.84	0.11	13
	Green	0.97	0.06	6	Blue	0.74	0.10	13	0.74	0.12	16
	Blue	0.84	0.10	12	Cyan	0.82	0.04	5	0.82	0.05	6
	Purple	1.09	0.08	8	Yellow	1.36	0.09	7	1.13	0.04	3
RGB yellow (R+G)	Red	192	10	5	Red	204	20	10	199	29	15
	Orange	291	26	9	Green	144	24	17	150	17	11
	Green	209	13	6	Blue	146	19	13	142	18	12
	Blue	156	11	7	Cyan	267	22	8	240	12	5
	Purple	180	10	6	Yellow	256	11	4	272	24	9
Mean RGB Luminosity***		110–147				85–152			79–160		

* Standard deviation

** Coefficient of variation=SD × 100 / Mean

*** (∑ luminosity for single rooftop)/number of roofs observed (5)

Table 3. Changes in normalized canopy spectral profile of *Ginkgo, Zelkova, Lithocarpus* and *Cedrus* canopies in the university campus

Tree species	Normalized spectral variable	2 Jun 2002		7 Dec 2003		15 Sep 2004		6 Jun 2010	
		Mean	SD*	Mean	SD	Mean	SD	Mean	SD
Ginkgo (n=3)	G	$70^{a\ B}$**	2	$107^{a\ A}$	4	$73^{a\ B}$	6	$72^{b\ B}$	0
	R/G	$0.78^{b\ B}$	0.05	$1.18^{a\ A}$	0.02	$0.84^{b\ B}$	0.08	$0.58^{ab\ C}$	0.04
	RGB yellow (R+G)	$124^{a\ BC}$	6	$235^{a\ A}$	10	$134^{a\ B}$	12	$114^{b\ C}$	2
Zelkova (n=2)	G	$39^{d\ C}$	2	$67^{b\ A}$	2	$51^{b\ B}$	6	$47^{d\ C}$	2
	R/G	$0.88^{a\ B}$	0.06	$1.22^{a\ A}$	0.02	$0.97^{a\ B}$	0.03	$0.55^{b\ C}$	0.08
	RGB yellow (R+G)	$74^{c\ C}$	5	$149^{b\ A}$	6	$99^{b\ B}$	13	$74^{c\ C}$	7
Lithocarpus (n=3)	G	$56^{c\ B}$	3	$62^{b\ B}$	8	$58^{b\ B}$	3	$120^{a\ A}$	1
	R/G	$0.86^{ab\ A}$	0.02	$0.90^{b\ A}$	0.04	$0.84^{b\ A}$	0.02	$0.66^{a\ B}$	0.04
	RGB yellow (R+G)	$104^{b\ B}$	5	$119^{c\ B}$	18	$107^{b\ B}$	7	$198^{a\ A}$	4
Cedrus (n=2)	G	$63^{b\ A}$	2	$64^{b\ A}$	4	$62^{ab\ A}$	2	$65^{c\ A}$	4
	R/G	$0.71^{b\ B}$	0.01	$0.89^{b\ A}$	0.01	$0.84^{b\ A}$	0.05	$0.64^{ab\ B}$	0.02
	RGB yellow (R+G)	$108^{b\ AB}$	2	$120^{bc\ A}$	8	$115^{ab\ AB}$	1	$106^{b\ B}$	5
Mean RGB luminosity***		130		87		119		131	

* Standard deviation

** For each time point and each color variable, the means indexed by the same small letter do not differ significantly among the tree species at $p=0.05$ according to the LSD *t*-test. For each color variable and each tree species, the means indexed by the same capital letter do not differ significantly among the time points at $p=0.05$ according to the *t*-test.

*** (∑ luminosity for rooftop) / number of rooftops observed (5)

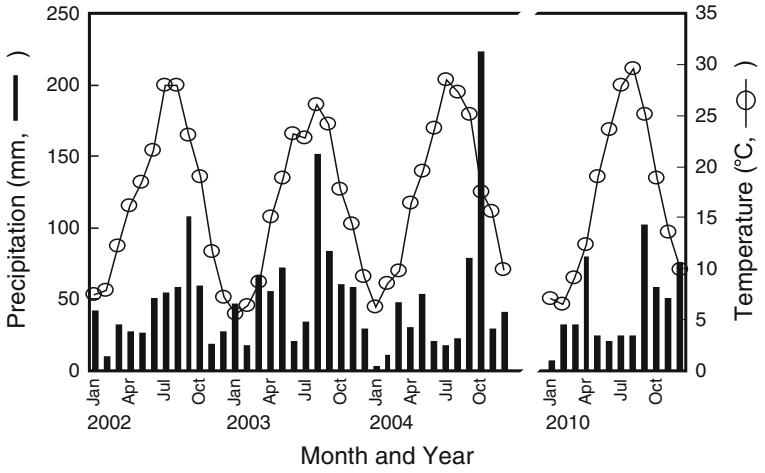

Figure 2. Temperature and precipitation in Tokyo in 2002, 2003, 2004 and 2010, in which the remote sensing images of the canopies were acquired.

(figure 2) were reflected in the canopy's spectral profiles (figure 1). *Ginkgo* leaves became bright yellow in December (figure 1a) when the normalized RGB yellow value exceeded 200, as the temperature dropped. As chlorophyll synthesis stops in *Ginkgo* leaves, the chlorophyll already present begins to decompose. The autumn breakdown of chlorophyll unmasks the relatively more stable yellow carotene and xanthopyll pigments, resulting in clear yellow-coloured leaves (Mori *et al.* 2000). On the same day, 7 Dec 2003, the *Zelkova* leaves were reddish brown, as indicated by the R/G value of 1.22. Although this value was not significantly different from that for the *Gingko* leaves (1.18), the lower intensity of both R and G made the spectral profile darker than the *Gingko* leaves (Equation 1). Unlike *Ginkgo* leaves, *Zelkova* is known to retain a red pigment called anthocyanine (Pallardy 2008). The *Lithocarpus* canopy exhibited another trend, an intensive yellowish green in early June 2010 (figure 1b), but not in the same season in 2002 (table 3). The cause of this specific spectral profile for the June 2010 time point was caused by the flowers that largely covered the leaves of this evergreen species, which usually flowers within May in the region (Okamoto 1989). In 2010, the total effective temperature (Σ [daily mean temperature −5°C, 5°C, or lower regarded as 0°C]) from 1 Feb to 30 Apr was just 409°C, while it was 602°C in the relatively warmer year of 2002 (figure 2). The total effective temperature for the period is known to affect the timing of the budburst of *Lithocarpus* (Fujimoto 2007). The delay in the development of new leaves and branches was thought to be responsible for the late flowering in 2010 (figure 1b). Among the canopies of the four species, the *Ginkgo* canopy had the lightest spectral profile in early (June) to late (September) summer. The *Zelkova* leaves were the darkest in early summer. This was likely due to its high chlorophyll concentration, as in the case of *Acacia auriculiformis*, a dark leaf species (Doi and Ranamukhaarachchi 2010), which has a high chlorophyll content (Prior *et al.* 2004). The canopy of the evergreen boreal tree *Cedrus* retained a low intensity value of G, indicating a constant dark green needle colour. The increase in redness in September to December was thought to be due to the small brownish flowers on the branches (Khanduri and Sharma 2010).

3.4 *Perspective*

The results presented above demonstrate the applicability of this normalization technique in the spectral profiling of leaves over a period of time. In actual fields, the leaf colours of both healthy and unhealthy plants may vary nonlinearly with time. Therefore, repeated observations of a spatially uneven distribution of greenness, yellowness and relative redness at multiple time points are expected to statistically separate the temporal (Summy and Little 2008) and spatial (Doi and Ranamukhaarachchi 2009) effects on the changes in leaf spectral profiles. The statistical separation of factors that affect leaf colour would thus clarify the spatial distribution patterns of abnormal leaf colour. This type of information should assist in identifying the cause of the abnormality. Because of the spatial unevenness and irregularity in plant disease (Nandris *et al.* 1985), fertilizer requirements (Doi and Ranamukhaarachchi 2009) and weed distribution (Pollnac *et al.* 2008), in addition to temporal changes, this normalization technique is worth considering, testing, improving and developing in various related activities. The normalization technique herein involves three spectral

variables. This is an advantage because the variables reveal multiple aspects related to the physiological status of plants. For general and public use, various freeware, such as GIMP, currently exist for the determination of the intensity values of RGB and other colour components for pixels in digital images. Such freeware will maximize the number of users. For more timely, precise and public use in the management of crops and other plant species, the current technique may form a practical combination with recently developed aerial photography methods, such as balloons with remotely controlled digital cameras (Verhoeve 2009), in addition to the most advanced remote sensing technologies.

References

Adams ML, Philpot WD and Norvell WA 1999 Yellowness index: an application of spectral second derivatives to estimate chlorosis of leaves in stressed vegetation. *Int. J. Remote Sens.* **20** 3663–3675

Balasubramanian V, Morales AC, Cruz RT, Thiyagarajan TM, Nagarajan R, Babu M, Abdulrachman S and Hai LH 2000 Adaptation of the chlorophyll meter (SPAD) technology for real-time N management in rice: A review. *Intl. Rice Res. Notes* **25** 4–8

Bunting P and Lucas R 2006 The delineation of tree crowns in Australian mixed species forests using hyperspectral compact airborne spectrographic imager (CASI) data. *Remote Sens. Environ.* **101** 230–248

Coste S, Baraloto C, Leroy C, Marcon E, Renaud A, Richardson AD, Roggy JC, Schimann H, Uddling J and Herault B 2010 Assessing foliar chlorophyll contents with the SPAD-502 chlorophyll meter: a calibration test with thirteen tree species of tropical rainforest in French Guiana. *Ann. For. Sci.* **67** 607

Doi R 2012 Quantification of leaf greenness and leaf spectral profile in plant diagnosis using an optical scanner. *Cienc. Agrotec.* **36** 309–317

Doi R and Mahaut S 2006 Effect of extract of *Curcuma alismatifolia* inoculated with *Ralstonia solanacerum* and cultured in vitro on detection of the bacterium using a medium: a case study. *Rev. Cienc. Agr.* **29** 241–252

Doi R and Ranamukhaarachchi SL 2009 Correlations between soil microbial and physicochemical variations in a rice paddy: implications for assessing soil health. *J. Biosci.* **34** 969–976

Doi R and Ranamukhaarachchi SL 2010 Discriminating between canopies of natural forest and acacia plantation plots in a Google Earth Image to evaluate forest land rehabilitation by acacia species. *Intl. J. Agric. Biol.* **12** 921–925

Doi R, Wachrinrat C, Teejuntuk S, Sakurai K and Sahunalu P 2010 Semiquantitative color profiling of soils over a land degradation gradient in Sakaerat, Thailand. *Environ. Monit. Assess.* **170** 301–309

Fujimoto S 2007 Analysis of prediction methods for budburst days based on the phenological observation in 29 broad-leaved tree species for 10 years. *J. Jpn. For. Soc.* **89** 253–261

Hadjimitsis DG, Clayton CR I and Retalis A 2009 The use of selected pseudo-invariant targets for the application of atmospheric correction in multi-temporal studies using satellite remotely sensed imagery. *Intl. J. Appl. Earth Obs.* **11** 192–200

Handschuh S, Schwaha T and Metscher BD 2010 Showing their true colors: a practical approach to volume rendering from serial sections. *BMCDev. Biol.* **10** 41

Hayes DJ and Sader, SA 2001 Comparison of change-detection techniques for monitoring tropical forest clearing and vegetation regrowth in a time series. *Photogramm. Eng. Rem. S.* **67** 1067–1075

Khanduri VP and Sharma CM 2010 Male and female reproductive phenology and annual production of male cones in two natural populations of *Cedrus deodara*. *Nordic J. Bot.* **28** 119–127

Kirk K, Andersen HJ, Thomsen AG, Jorgensen JR and Jorgensen RN 2009 Estimation of leaf area index in cereal crops using red-green images. *Biosystems Eng.* **104** 308–317

Kondo N, Ahmad U, Monta M and Murase H 2000 Machine vision based quality evaluation of Iyokan orange fruit using neural networks. *Comput. Electron. Agric.* **29** 135–147

Lev-Yadun S and Gould KS 2007 What do red and yellow autumn leaves signal? *Bot. Rev.* **73** 279–289

Lu D and Weng Q 2007 A survey of image classification methods and techniques for improving classification performance. *Intl. J. Remote Sens.* **28** 823–870

Mori M, Suzuki K and Kohzaki R 2000 Variations in chlorophyll and carotenoid content in the growth process of the Ginkgo leaf. *J. Jpn. Soc. Food Sci. Technol.* **47** 448–451

Nandris D, Vancanh T, Geiger JP, Omont H and Nicole M 1985 Remote-sensing in plant-diseases using infrared color aerial-photography - applications trials in the Ivory Coast to root diseases of *Heveabrasiliensis*. *Eur. J. For. Pathol.* **15** 11–21

Newton A, Hill R, Echeverria C, Golicher D, Benayas J, Cayuela L and Hinsley S 2009 Remote sensing and the future of landscape ecology. *Prog. Phys. Geog.* **33** 528–546

Okamoto M 1989 A comparative study of the ontogenetic development of the cupules in *Castanea* and *Lithocarpus* (*Fagaceae*). *Pl. Syst. Evol.* **168** 7–18

Olszewska M, Grzegorczyk S, Alberski J, Baluch-Malecka A and Kozikowski A 2008 Effect of copper deficiency on gas exchange parameters, leaf greenness (SPAD) and yield of perennial ryegrass (*Lolium perenne* l.) and orchard grass (*Dactylis glomerata* l.). *J. Elementol.* **13** 597–604

Pagani A, Echeverria HE, Andrade FH and Rozas HR S 2009 Characterization of corn nitrogen status with a greenness index under different availability of sulfur. *Agron. J.* **101** 315–322

Pallardy SG 2008 *Physiology of woody plants 3rd ed*. (Burlington, Ma.: Academic Press)

Pollnac FW, Rew LJ, Maxwell BD and Menalled FD 2008 Spatial patterns, species richness and cover in weed communities of organic and conventional no-tillage spring wheat systems. *Weed Res.* **48** 398–407

Prior L, Bowman D and Eamus D 2004 Seasonal differences in leaf attributes in Australian tropical tree species: family and habitat comparisons *Funct. Ecol.* **18** 707–718

Schott JR, Salvaggio C and Volchok WJ 1988 Radiometric scene normalization using pseudoinvariant features. *Remote Sens. Environ.* **28** 1–16

Shuvalov VA 2007 Electron and nuclear dynamics in many-electron atoms, molecules and chlorophyll-protein complexes: A review. *BBA-Bioenergetics* 1767 422–433

Sicher RC 1999 Photosystem-II activity is decreased by yellowing of barley primary leaves during growth in elevated carbon dioxide. *Intl. J. Plant Sci.* **160** 849–854

Smith, B. 1999 An RGB to spectrum conversion for reflectances. *J. Graph. Tools* 4 11–22

Spurr SH 1948 *Aerial photographs in forestry* (New York: Ronald Press)

Steele MR, Gitelson AA and Rundquist DC 2008 A comparison of two techniques for nondestructive measurement of chlorophyll content in grapevine leaves. *Agron. J.* **100** 779–782

Summy KR and Little CR 2008 Using color infrared imagery to detect sooty mold and fungal pathogens of glasshouse-propagated plants. *HortScience* **43** 1485–1491

Van Niel TG and McVicar TR 2004 Current and potential uses of optical remote sensing in rice-based irrigation systems: a review. *Aust. J. Agric. Res.* **55** 155–185

Verhoeve GJJ 2009 Providing an archaeological bird's-eye view – an overall picture of ground-based means to execute low-altitude aerial photography (LAAP) in archaeology. *Archeol. Prospect.* **16** 233–249

Yang Z, Willis P and Mueller R 2008 Impact of band-ratio enhanced AWIFS image to crop classification accuracy. *Proc. Pecora* **17** *http://www.asprs.org/a/publications/proceedings/pecora17/0041.pdf*

MS received 10 May 2011; accepted 21 June 2012

Corresponding editor: UTPAL NATH